

High-pressure hydriding of Zircaloy cladding by the thermogravimetry and tube-burst techniques

Hyun Seon Hong ^{a,*}, Lembit Sihver ^b, D.R. Olander ^c, L. Hallstadius ^d

^a *Plant Engineering Center, Institute for Advanced Engineering, Yongin 449-863, Republic of Korea*

^b *Department of Materials and Surface Chemistry, Nuclear Science and Technology, Chalmers University of Technology, SE-412 96, Sweden*

^c *Department of Nuclear Engineering, University of California, Berkeley, CA 94720, USA*

^d *Westinghouse Atom AB, SE-721 63 Västerås, Sweden*

Received 18 May 2004; accepted 14 September 2004

Abstract

Hydriding kinetics of modified Zircaloy claddings was studied by the thermogravimetric method at 400°C and the tube-burst technique at 315°C. Some specimens were prefilmed with a thin oxide layer by air oxidation on both the inner and outer surfaces which were either pickled or blasted. In the thermogravimetric test, the hydriding rates of bare cladding specimens (no oxide prefilm) were in the range 0.9–1.6 mg/cm²h with little effect of the surface treatment. Incubation times were less than 1 h or even zero. In the tube-burst test, immediate and extensive hydrogen uptake was observed for these non-coated specimens. On the other hand, the cladding specimens with oxide prefilm exhibited lower hydriding rates ranging from 0.01 to 0.05 mg/cm²h and incubation times increased to 42 h. In addition, no hydrogen uptake was observed for all oxide-coated specimens for 100–750 h.

© 2004 Elsevier B.V. All rights reserved.

1. Introduction

In a failed fuel element, oxidation of the cladding inner surface by steam produces hydrogen in the fuel-cladding gap. Hydrogen formation may be enhanced by fission fragment recoil from the fuel into the gap, where water is decomposed into hydrogen and oxygen [1]. Hydrogen eventually penetrates the oxide scale on the cladding inner surface and forms zirconium hydride in the metal. This process can cause secondary cladding

failure, manifest by axial splitting due to large hoop stress in the hydrided metal or by hydride blisters or bulges which can lead to small cracks or circumferential breaks that will expose fuel to the coolant [2–4]. Consequently, considerable effort is devoted to development of advanced cladding materials that exhibit both improved waterside corrosion resistance and resistance of internal surfaces to local massive hydriding in a steam-starved environment. An important component of a development program for advanced cladding alloys is a method of testing the candidate materials for resistance to hydrogen attack.

The microbalance method (the thermogravimetric method) is a well-established technique for measurement of Zircaloy hydriding kinetics [5–12]. Because the measurement responds to global hydriding, the effect of

* Corresponding author. Tel.: +82 31 330 7481/222 90 0382; fax: +82 31 330 7113/222 82 4914.

E-mail address: hshong@iae.re.kr (H.S. Hong).

intentional flaws in the specimen can be studied. However, the experimental conditions of the microbalance tests differ from those in-reactor. Specimen geometries other than tubing and the inability to simulate the temperature gradient through the cladding and the pressure differential across the tube prevent reproduction of in-reactor conditions. However, the temperature range studied and the reproduction of the total hydrogen pressure in failed BWR fuel elements provide sufficient information on the basic kinetics of the reaction, which should apply to reactor operating conditions.

The 'tube-burst' test is a recently developed laboratory technique that provides a complementary measure of the resistance of Zircaloy (Zry) cladding to attack by hydrogen [13,14]. The method involves a closed tube specimen with initially equal high pressures inside (H_2) and outside (He) the tube so that the pressure conditions of a failed fuel rod during reactor operation are closely simulated. The time to rupture of the cladding specimen is the principal measurement. This method avoids the edge effect that causes difficulties in the thermogravimetric test method. Both the thermogravimetric and the tube-burst methods utilize realistic pressures (70 bar), thereby avoiding the atypical atmospheric or sub-atmospheric pressures used in the previous laboratory experiments [15–17].

This work is part of a program sponsored by former ABB Atom AB (currently Westinghouse Atom AB) intended to obtain the hydriding characteristics of modified Zircaloy. The objective is to investigate the effect of ID surface coatings or laboratory treatment on the resistance of Zircaloy to attack by high-pressure hydrogen and hydrogen-steam mixtures.

2. Experimental

2.1. High-pressure microbalance

Zircaloy claddings (ID = 0.85 cm) were prepared in the present study. Some tubing specimens have $\approx 70 \mu\text{m}$ thick Zr–Sn alloy liner on the inner surface. Some lined specimens were prefilmed with a thin oxide layer by air oxidation on both the inner and outer surfaces which were either pickled or blasted. Specimen designations, descriptions and experimental conditions are summarized in Table 1. Zircaloy tubing was cut into 1-cm long pieces in order to fit into the microbalance furnace tube. The microbalance apparatus used to measure in-situ specimen weight changes due to reaction with hydrogen/steam is shown in Fig. 1. The specimen chamber is vertically connected to the microbalance chamber by

Table 1
Summary of the microbalance test results (400 °C, 70 bar H_2)

Specimen	Description	Maximum hydriding rate (mg/cm^2)	Average hydriding rate (mg/cm^2)	Incubation time (h) ^a	Test condition
BZOL	Zry with blasted liner (blasted with zirconium oxide)	0.93	0.61	0	A ^b
PL					
(-1)	Zry with pickled liner	1.37	0.78	3/4	A
(-2)		1.56	1.03	0	A
BSCM					
(-1)	Zry mono tube, blasted	1.37	0.70	0	A
(-2)	(blasted with silicon carbide)	1.60	1.46	0	A
BZOM					
(-1)	Zry mono tube, blasted	1.44	–	3/4	A
(-2)	(blasted with zirconium oxide)	1.48	0.67	0	A
PM					
(-1)	Zry mono tube, pickled	3.80	1.18	0	A
(-2)		0.55	0.55	0	A
BZOL-O	BZOL + air oxidation (3–5 μm ZrO_2)	0.01	–	42	B ^c
PL-O	PL + air oxidation (3–5 μm ZrO_2)	0.05	–	20	A
PL-A	PL + autoclaved (8–10 μm ZrO_2)	0.01	–	8	B

^a Before massive hydriding.

^b 400 °C and 70 bar dry H_2 .

^c 400 °C and 70 bar H_2 with water vapor supplied from a room temperature-water reservoir for a certain period of time before switching the reaction chamber to dry hydrogen.

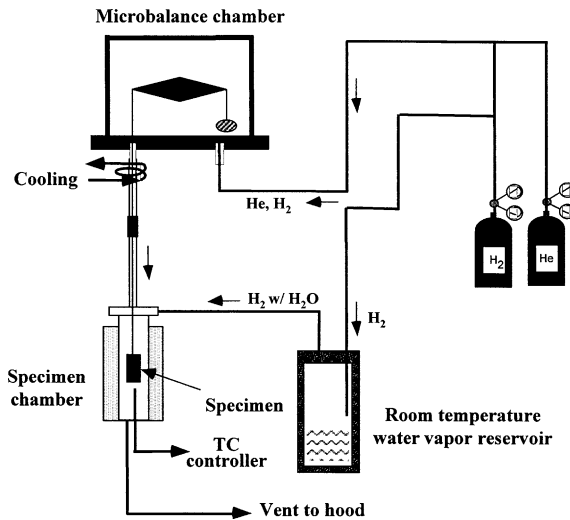


Fig. 1. Schematic diagram of microbalance experimental setup.

the hang-down tube. To avoid the deleterious effect of corners on hydrogen uptake, both ends of the tube were sealed with aluminum caps with liquid indium protection. The microbalance chamber is placed on a steel frame. The upper end of the hang-down tube is water-cooled to avoid heating of the microbalance. To prevent ingress of steam from the specimen chamber into the microbalance chamber, high-pressure carrier gas flows first through the microbalance chamber, and then passes down the hang-down tube, through the specimen chamber before exiting at the bottom of the specimen chamber. The specimen chamber is 50 mm long and 16 mm inside diameter.

Commercial grade hydrogen is pressure-regulated to 70 bar and flows at a rate of 0.51 (STP) per minute into the specimen chamber and the hot zone of the furnace. The specimen is suspended by a platinum wire from the arm of the microbalance. The hot zone of the furnace is heated to 400 °C, and the weight gain change due to hydrogen uptake is monitored during the experiment.

Within an hour of the start of the test, the water content of the H₂ without added water vapor is <20 ppm. The hydriding environments applied in these experiments include

- (1) 400 °C and 70 bar dry H₂ (experimental condition; A)
- (2) 400 °C and 70 bar H₂ with water vapor supplied from a room temperature-water reservoir for a certain period of time before switching the reaction chamber to dry hydrogen. The steam content of the H₂ entering the reaction chamber from the reservoir is ≈500 at-ppm (experimental condition; B).

2.2. Tube-burst test

Specimens are 30 cm long with a wall thickness of 0.63 mm. To eliminate the effect of corners, only the 2.5-cm center portion was heated. Consequently, a temperature gradient along the length of the Zry tube is unavoidable. The temperature profile, however, can be characterized before the experiment using thermocouples. Preliminary results showed that this gradient has little effect on the hydrogen uptake of the heated zone. All the hydriding, observed post-test by visual examination of the ruptured tube, occurred nearly exclusively at the heated zone.

The experimental setup for the tube-burst test (Fig. 2) consists of a reaction chamber, two pressure transducers and a water supply. All tests were conducted at 315 °C. The test was terminated when the specimen failed, as indicated by a sudden equalization of the inner and outer pressures. If no failure occurred, the test was terminated after 100–750 h.

The hydriding experiments were conducted in a stag-

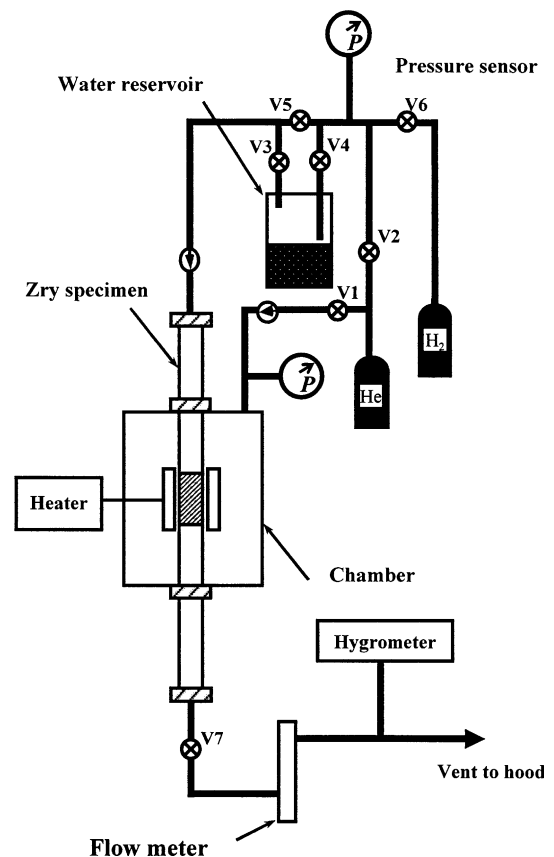


Fig. 2. Schematic diagram of the tube-burst experimental setup.

nant gas. The inside of the tube and the outer chamber were pressurized first with pure helium by opening the valves V1, V2 and V5 in Fig. 2 and by closing valve V7. After pressurizing, the system was sealed by closing the valves V1 and V2. The center portion of the Zry tube was heated to the desired temperature, and the leak rate of the specimen under these conditions was recorded for more than 20h. If no leak was found, the helium gas inside the specimen was purged by opening V7 and replaced with hydrogen at 70bar by opening V6 and closing V7. The hydrogen endurance test was started by closing V6, which isolates the specimen from its gas supply. The fixed amount of available hydrogen (6.2×10^{-2} mol) exceeds that required to completely convert the 2.5cm long hot section to $ZrH_{1.63}$ (3.5×10^{-2} mol).

3. Results and discussion

3.1. Microbalance experiments

Table 1 summarizes the conditions and hydriding rates for all experiments. All were conducted at 400°C and 70bar H_2 pressure. Fig. 3 shows typical

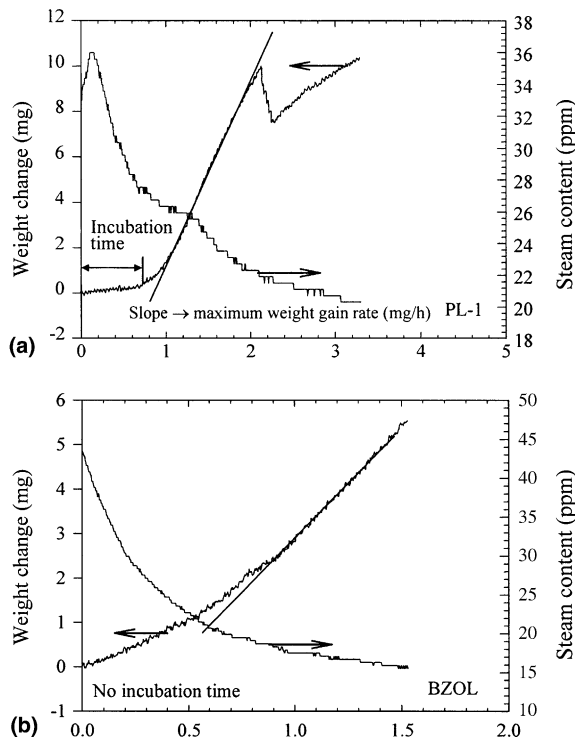


Fig. 3. Typical hydriding curves of non-oxide-coated specimens obtained from the microbalance test: (a) with an incubation time, (b) without an incubation time.

hydriding curves of non-oxide-coated specimens obtained from the microbalance test: (a) with an incubation time, (b) without an incubation time. As shown in Fig. 3(a), the PL-1 specimen started to hydride in less than 1 h. The BZOL specimen (Fig. 3(b)) was hydrided almost immediately. Visual examination of the specimen showed that the exposed surface was uniformly hydrided.

The average hydriding rates, the maximum hydriding rates and rough estimates of the incubation times are presented in Table 1. The average hydriding rate is the total weight gain per the test duration and the unit surface area, and the maximum hydriding rate is the maximum weight gain rate per unit surface area as shown in Fig. 3. In most tests, the specimen gained weight slowly at first and the rate accelerated thereafter. This phenomenon may be caused by the inhibiting effect of the high-initial water content of H_2 as seen in Fig. 3. Generally, incubation times are less than an hour or even zero. The maximum hydriding rates for most specimens except the PM specimen were about $1.4 \text{ mg/cm}^2\text{h}$, with little effect of cladding type and surface treatment. The PM specimen showed some scattered data. The lowest maximum hydriding rate was $0.93 \text{ mg/cm}^2\text{h}$ in the BZOL specimen and the highest was $1.60 \text{ mg/cm}^2\text{h}$ in the BSCM specimen. In the case of the average hydriding rate, the average rates were about $0.8 \text{ mg/cm}^2\text{h}$ for most specimens. The lowest rate was $0.61 \text{ mg/cm}^2\text{h}$ in the BZOL specimen and the highest was $1.46 \text{ mg/cm}^2\text{h}$ in the BSCM specimen, similarly to the maximum hydriding rate.

Fig. 4 shows typical hydriding curves of oxide-coated specimens obtained from the microbalance test: (a) PL-A hydrided by water vapor contained hydrogen and (b) PL-O hydrided by 'dry' hydrogen. For the oxide-prefilmed specimens (BZOL-O and PL-A) except PL-O, the test procedure consists of exposing the specimen to H_2 with 500-ppm water vapor for 72h then switching to dry hydrogen. These specimens did not hydride during the period when the H_2 contained 500-ppm steam. One specimen had scratches on the surface but these healed, when exposed to H_2 with 500-ppm water vapor. After purging with dry hydrogen, specimens PL-A (Fig. 4(a)) and BZOL-O hydrided with the incubation times of 8 and 42h, respectively. Fig. 4(b) shows that the PL-O specimen hydrided by dry hydrogen had 20-h incubation time indicating that the prefilm is protective in pure hydrogen and the maximum hydriding rate was $0.05 \text{ mg/cm}^2\text{h}$ after the incubation. For oxide-prefilmed specimens, the maximum hydriding rates were in the range $0.01\text{--}0.05 \text{ mg/cm}^2\text{h}$ in dry hydrogen. These rates are much lower than those specimens with no oxide layer. An oxide layer on the surface of Zry cladding, whether produced by air oxidation or autoclaving in steam, significantly slows the hydriding

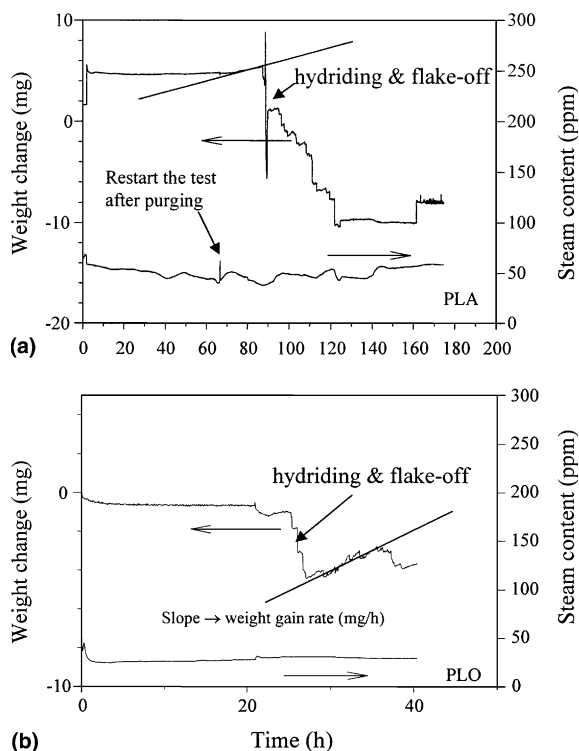


Fig. 4. Typical hydrating curves of oxide-coated specimens obtained from the microbalance test: (a) PL-A hydrated by hydrogen containing water vapor, (b) PL-O hydrated by 'dry' hydrogen.

reaction, and moderately increases the incubation time in pure H_2 .

3.2. Tube-burst experiments

Fig. 5 shows the pressure traces in the tube-burst experiment using a BSCM specimen. It is typical of all such plots in this series of tests. The specimen was first subjected to 70 bar helium pressure (inside the tube) and 69 bar helium in the reaction chamber. During heating the specimen at about 315°C , no pressure decrease was found for about 19 h as shown in Fig. 5(a).

The gas inside the tube was then switched to H_2 at 70 bar. The pressure inside the tube started to decrease as soon as the test resumed. The hydrided specimen failed in 52 min, as evidenced by equalization of the pressure between the inside and outside of the tube (Fig. 5(b)). Visual examination of the hydrided tube showed that most hydrogen uptake occurred at the center of the 2.5 cm long heated zone. The drop in H_2 pressure from its initial value to the value at failure (Δp_{H_2}) ranged from 7.6 to 13 bar. The hydrogen content at failure, cal-

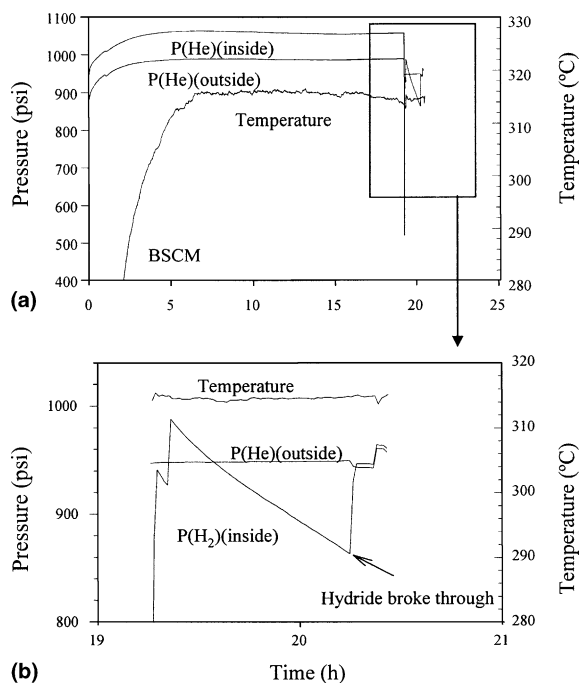


Fig. 5. Plots of pressure vs. time for a failed specimen obtained from tube-burst experiment: (a) result of the tube-burst experiment using BSCM specimen, (b) continuation of the result of BSCM, 1000 psi \approx 69 bar.

culated from Eq. (1), was in the range 4500–7800 wt-ppm.

$$n_H = 2 \frac{\Delta p_{H_2}}{R} \left(\frac{V_h}{T_h} + \frac{V_c}{T_c} \right), \quad (1)$$

where n_H is the number of gram-atoms of hydrogen absorbed, V_c the volume of the cold portion of the specimen ($\approx 16 \text{ cm}^3$), V_h the volume of the heated portion ($\approx 1.5 \text{ cm}^3$), R (82 bar $\text{cm}^3/\text{mol K}$) the universal gas constant and Δp_{H_2} the hydrogen pressure drop to failure in bar. The temperature of the hot zone is 315°C and the cold average temperature is 20°C .

A summary of the results of the tube-burst experiments is presented in Table 2. The time to failure, the hydrogen absorbed, and the failure mode are listed. All oxide-prefilmed specimens survived the test. Among the uncoated specimens (runs 1–7), only one cladding type (PL) survived more than 100 h in dry H_2 at the average hot-zone temperature of about 315°C . Five specimens failed in 3 h or less, and one specimen (BZOL) failed 3 h after a restart following a 23-h test with no failure. PL and PM in which inner surfaces were etched showed the different behavior in the tube-burst experiments. PL survived over 100 h while PM immediately hydrided and failed after the 1-h exposure to H_2 . Not enough tests were performed to characterize accurately the

Table 2
Summary of the results of the tube-burst experiments

Runs	Specimen type	Time to failure (min)	Hydrogen absorption ^b (wtppm)	Fracture mode ^a
Run-1	BZOL	1550	≈2100	≈20°
Run-2	PL		Not failed (tested up to 120h)	
Run-3	BSCM	52	≈4500	≈40°
Run-4	BZOM	60	≈6100	≈40°
Run-5	PM	62	≈5900	≈40°
Run-6	REF1	185	≈7800	Hole
Run-7	BSCL ^c	120	≈5600	Hole
Run-8	BSCL-O ^d		Not failed (tested up to 750h)	
Run-9	BZOL-O		Not failed (tested up to 100h)	
Run-10	PL-O		Not failed (tested up to 160h)	

^a The angles listed are with respect to the angular cross section normal to the tube axis.

^b Based on a 2.5 cm heated length.

^c Zry with blasted liner (blasted with silicon carbide).

^d BSCL + air oxidation (3–5 μm ZrO₂).

hydriding behavior of the etched samples in this study. The relevance of the etching effect to the hydrogen pick-up remains to be demonstrated. However, it was reported that chemically etching of Zircaloy could provide immunity from hydrogen uptake for a certain amount of time. The reason for the immunity was ascribed to a relatively clean metal surface and the newly formed protective oxide layer [13,14]. A thin native oxide exists on the inner surface of the as-received cladding material. This oxide layer could have imperfections such as small cracks or scratches, which allowed hydrogen permeation through the layer during testing. However, etching provides the less defect metal surface and the new oxide layer formed on it during testing is protective, thereby enhancing hydriding resistance.

Visual examination of the failed specimens showed that ≈0.7 cm at the center of the hot zone was completely hydrided and crumbled (see Fig. 6). The fracture surface was inclined at about 40° with respect to normal to the axial direction. The failure mode in runs 1–5 is circumferential (i.e., the tube broke into two parts). The

edges of the remaining specimen beyond the hot zone were mostly metallic. It appeared as if hydriding of the entire wall cross section had started at the hot center and progressed axially in both directions. The 20°–40° angle of the failed surface shown in Table 2 may be due to misalignment of the heating element, which surrounds the center of the specimen; if one side of the tube is shifted up or down, part of the heater can touch the tube and cause a circumferential temperature gradient in addition to the predominant axial temperature gradient. However, consistent angles of inclination of the fracture suggest that the cause of the inclination be the preferred orientation of the Zry in the tubing.

Two of the specimens failed forming a hole in the 2.5-cm hot zone. This hole was probably made after an elliptical hydrided portion of the tube wall popped out. The hole represents the loss of the hydride before the entire circumference has been reacted. The sizes of holes ranged from one-third to a half of the hot zone. Besides, it was observed that the remaining region in the hot zone from the popped-out portion was uniformly hydrided. Consequently, it is assumed that the pick-up takes place uniformly across the whole surface area of the hot zone.

For the oxide-coated specimens (runs 8–10 in Table 2), no hydrogen absorption was observed and all the specimens survived for 100–750 h at the average hot-zone temperature of about 315°C. Examination after the test showed no hydriding of the hot zone of the specimen. Thus, the oxide-coated specimens withstand chemical attack by hydrogen at 315°C.

4. Conclusions

Both the microbalance and tube-burst tests showed that bare Zircaloy cladding failed rapidly in dry hydrogen at 70 bar pressure and temperatures of 400°C

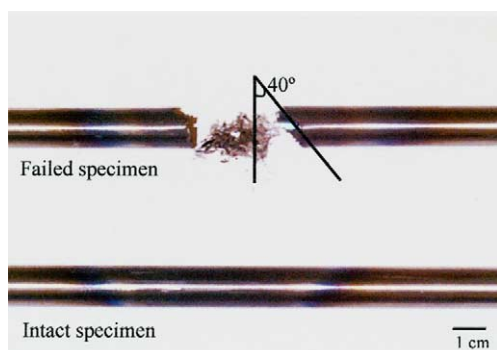


Fig. 6. Shape of the failed specimen in the tube-burst experiment.

(microbalance) or 315°C (tube-burst). Blasting the surface with various types of grits did not improve resistance to attack by hydrogen. On the other hand, prefilming the surface of the cladding with $\approx 4\mu\text{m}$ of ZrO_2 provided excellent protection against hydriding in both types of tests. In addition, these specimens were exposed to hydrogen with 500 ppm H_2O for 72 h. This treatment did not compromise the hydriding resistance, and may even have rendered the prefilm more protective. The ID of cladding in reactor service can acquire an oxide coat up to $\approx 10\mu\text{m}$. However, this scale does not provide protection against massive hydriding in a failed fuel element. Both types of tests provide excellent means of assessing the hydrogen resistance of newly developed cladding. The tube-burst method is the simpler of the two, and should be a routine part of the development program for advanced zirconium-based cladding.

References

- [1] C.Y. Li, D.R. Olander, *Rad. Phys. Chem.* 54 (1999) 301.
- [2] J.C. Clayton, in: *Proc. Eighth International Symposium on Zirconium in the Nuclear Industry*, ASTM STP 1023, 1989, p. 266.
- [3] D.R. Olander, S. Vaknin, Secondary hydriding of defected Zircaloy-clad fuel rods, Report EPRI TR-101773, 1993.
- [4] R.L. Yang, O. Oze, S.K. Yagnik, B. Cheng, H.H. Klepfer, N. Kjaer-Pedersen, et al. EPRI failed fuel degradation R&D program. In: *Proceedings of the International Topical Meeting on LWR Fuel Performance*, West Palm Beach, FL, USA, American Nuclear Society, 1994.
- [5] Y.S. Kim, W.-E. Wang, D.R. Olander, *High Temp.–High Press.* 27&28 (1995–1996) 555.
- [6] Y.S. Kim, W.-E. Wang, D.R. Olander, S.K. Yagnik, *J. Nucl. Mater.* 246 (1997) 43.
- [7] D.R. Olander, W.-E. Wang, Y.S. Kim, C.Y. Li, S. Lim, S.K. Yagnik, *J. Nucl. Mater.* 248 (1997) 214.
- [8] Y.S. Kim, W.-E. Wang, D.R. Olander, S.K. Yagnik, *J. Nucl. Mater.* 240 (1996) 27.
- [9] Y.S. Kim, W.-E. Wang, D.R. Olander, S.K. Yagnik, *J. Nucl. Mater.* 245 (1997) 152.
- [10] R.P. Marshall, *J. Less-Common Met.* 13 (1967) 45.
- [11] S. Aronson, Some experiments on the permeation of hydrogen through oxide films on Zirconium, Report WAPD-BT-19, 1960.
- [12] K. Une, *J. Less-Common Met.* 57 (1978) 93.
- [13] H.S. Hong, W.E. Wang, D.R. Olander, High pressure hydriding of Zircaloy cladding by the tube-burst technique. In: *International Topical Meeting on LWR Fuel Performance*, Park City, UT, American Nuclear Society, 2000.
- [14] H.S. Hong, D.R. Olander, *J. Nucl. Mater.* 297 (2001) 107.
- [15] D.W. Shannon, *Corrosion* 19 (1963) 414.
- [16] R.L. Gibby, Hydriding of PRTR fuel rod end caps, Report BNWL 150, 1965.
- [17] R.F. Boyle, T.J. Kisiel, Hydrogen permeation of Zircaloy-2 corrosion films, Report WAPD-BT-10, 1958.